Asian Journal of Chemistry; Vol. 37, No. 11 (2025), 2733-2737
ASIAN JOURNAL OF CHEMISTRY
https://doi.org/10.14233/ajchem.2025.34535

Transforming Aquatic Waste into Healing Agent: Sustainable Extraction, Characterization and Bioactivity of Chitosan from *Gibelion catla* Scales

CHITRALEKHA KATAKI[1,2], AJAIKUMAR B. KUNNUMAKKARA[3], MUKESH KUMAR MANICKASAMY[3], SMITA BARUAH[1] and MINAKSHI BHATTACHARJEE[1,*]

[1]Faculty of Science, Assam down town University, Sankar Madhab Path, Gandhi Nagar Panikhaiti, Guwahati-781026, India
[2]Faculty of Paramedical Science, Assam down town University, Sankar Madhab Path, Gandhi Nagar Panikhaiti, Guwahati-781026, India
[3]Cancer Biology Laboratory, Department of Biosciences and Bioengineering, Indian Institute of Technology Guwahati, Guwahati-781039, India

*Corresponding author: E-mail: minakshi.bhattacharjee@adtu.in

Received: 25 July 2025 *Accepted*: 15 September 2025 *Published online*: 27 October 2025 AJC-22160

Chitosan possesses innumerable implementations in the field of biomedical, pharmaceutical and industry. Chitin is an amino polysaccharide polymer occurring in the protective exoskeleton of fish, crustaceans, insects along with fungi, from which chitosan can be derived by deacetylation. This research aimed to extract chitosan from *Gibelion catla* scales and characterise it using Fourier transform infrared spectroscopy (FTIR), X-ray diffraction (XRD), scanning electron microscopy coupled with energy dispersive X-ray spectroscopy (SEM/EDX) and elemental analysis along with an investigation of antimicrobial activity, cytotoxicity and wound healing activity. The FTIR identified various functional groups associated with organic compounds such as O-H stretching at (3461 cm^{-1}), C=O stretching (1640 cm^{-1}), C-H bending (1471 cm^{-1}) and C-N stretching (1417 cm^{-1}), confirmed the presence of hydroxyl, carbonyl and amine functionalities typical of partially deacetylated chitosan. The degree of deacetylation was determined to be 60.4%, suggesting a moderate level of conversion from chitin to chitosan. X-ray diffraction (XRD) analysis revealed a semi-crystalline structure, with a prominent peak observed at 32.04º, which is indicative of the polymer's ordered crystalline nature. Scanning electron microscopy (SEM) further supported this, showing a rough, fibrillary surface morphology with visible porosity, which is consistent with the structural features observed in chitosan-based materials. Elemental profiling demonstrated that chitosan is rich in oxygen and calcium, phosphorus and carbon, which is attributed to residual inorganic content or interactions with mineral components, while the high oxygen and carbon content aligns with the organic polymeric nature of chitosan. Chitosan induced the formation of a measurable inhibition zone against all the bacterial species (*Escherichia coli*, *Bacillus subtilis* and *Staphylococcus aureus*) at all the tested concentrations. MTT analysis revealed that chitosan is strongly toxic to MDA MB-231 (triple negative breast cancer) cells and non-toxic to PSVK1 (normal skin keratinocytes). The scratch wound healing assay showed significant wound closure, indicating enhanced cell migration and regenerative activity. All these findings suggest that waste scales of *Gibelion catla* are prominent and rich sources of chitosan and the obtained product is biodegradable, antibacterial, naturally derived polysaccharide and can be employed as anticancer agent and wound dressing material.

Keywords: Chitosan, FTIR, XRD, SEM-EDX, Antimicrobial, Cytotoxicity, Wound healing.

INTRODUCTION

Chitosan is a native polycationic linear polysaccharide derived from chitin. Chitin is a straight chain biopolymer composed of 2-acetamide-2-deoxy-D-glucopyranose units joined by the β (1,4) glycosidic bond. Chitin, the naturally occurring polysaccharide, is the primary component of the cell wall in fungi, the exoskeletons of arthropods, for instance crustaceans and insects, the radulae of molluscs and is the second most popular biopolymer in nature after cellulose [1]. As highlighted by Varma & Vasudevan [2] unlike cellulose chitin has acetamide moieties attached at C–Z positions. On the ground of the source, chitin can establish two allomorphic forms (α and β), with α-chitin being abundantly present in the exoskeleton of shellfish, chiefly from shrimps and crabs [2]. Due to their unique physico-chemical and biological properties, chitin and its derivatives can serve as immunostimulants, anticoagulants, enzyme inhibitors, antimicrobials, anticancer agents, anticholesterolemic agents and wound repairing agents. They are also employed as biosorbents for the removal of metal ions from contaminated water. Chitosan, consisting of 2-amino-2-deoxy-D-glucopyranose units joined by β (1→4) glycosidic bonds,

can be extracted from chitin by deacetylation reaction through alkaline hydrolysis and subsequent treatment with acid solutions [3]. Owing to the existence of charged units, the chitosan molecule might be classified as predominantly an ampholyte or a polyelectrolyte [4].

Fish scales, rich in chitin, offer a cost-effective and eco-friendly source for chitosan extraction. Their reuse supports circular economy and waste valorization in aquaculture. Converting this waste into antimicrobial biopolymers holds promise for biomedical applications such as wound healing, drug delivery and tissue engineering, where biocompatible and non-toxic alternatives are increasingly in demand. Among various fish species, *Gibelion catla* (commonly known as Catla), a widely cultivated freshwater fish in South Asia, generates a substantial quantity of scale waste during processing, which remains largely unexploited.

Chitosan, a natural biopolymer, is used due to its biodegradability, biocompatibility, non-toxicity, renewability and natural abundance [5]. Unlike the synthetic polymers, it offers additional benefits such as antimicrobial activity, hydration, non-antigenicity and haemostatic effects [6]. Its chemical structure containing reactive hydroxyl (–OH) and amino ($–NH_2$) groups and a positive charge enables broad biological applications [7]. Chitosan extraction typically involves deproteinization, demineralization and deacetylation, with the source material significantly influencing the properties of the final product [8]. Therefore, this study aimed to extract and characterize chitosan from *Gibelion catla* fish scales and evaluate its antimicrobial, cytotoxic and wound healing properties. The goal was to assess its potential as a biodegradable, bioactive material for biomedical applications.

EXPERIMENTAL

Collection and preparation of sample: Scales of catla fish, Bhokua in Assamese (*Gibelion catla*), were collected from the local fishermen of Uzan Bazar, Guwahati, Assam (India) and brought to the laboratory for the extraction of chitosan. The fish scales were washed with fresh water several times to remove sand, dirt and all other wastes. The washed scales were then sun-dried for several days.

Extraction of chitosan: Chitosan was extracted from fish scale by using the standard protocol [8]. The fish scales were demineralized with 1% HCl. Dried fish scales (50 g) were immersed in HCl for 36 h to eliminate the minerals ($CaCO_3$ and $Ca_3(PO_4)_2$). Then, the scales underwent multiple washing with distilled water. Then deproteinization was done by immersing the demineralized scales in 0.5 N NaOH at ambient temperature for 18 h in order to separate proteins from the scales in order to obtain chitin. The extracted chitin was further deacetylated to obtain the chitosan. The process of deacetylation involved treatment with 50% NaOH and then heating for 2 h at 80 ºC in water bath. Afterward, the samples were repeatedly rinsed with water and filtered to isolate the solid residue, namely chitosan. To remove the residual moisture, the samples oven-dried. Following deacetylation, chitosan was recovered as a powder. The yield of chitosan was determined gravimetrically based on the dry weight difference between the raw fish scales and the final chitosan obtained. This was achieved by drying the fish scales and chitosan to a constant weight, thereby eliminating the influence of residual moisture on the weight difference [9].

Characterization: The FTIR analysis was analyzed with a Perkin-Elmer spectrometer (Model Spectrum RX I) using the Nujol method. To evaluate the crystalline structure and estimate the average crystallite size, X-ray Diffraction (XRD) analysis was carried out using Cu*K*α radiation at a standard scan rate of 1º min^{-1}. The surface morphology and structural features were examined using Scanning Electron Microscopy (SEM) on a TESCAN VEGA3 operated at 30 kV. Elemental composition was determined using Energy Dispersive X-ray Spectroscopy (EDX), with a carbon-coated copper grid employed to prevent interference from elemental peaks.

Biological activity

Antibacterial activity: Antimicrobial assay was done by agar well diffusion method against bacteria *viz.*, *Escherichia coli* (Gram-negative), *Staphylococcus aureus* and *Bacillus subtilis* (Gram-positive). The bacterial strains were collected from the microbiology laboratory of the down town Hospital, Guwahati and were sub-cultured. Bacterial inoculum was prepared by inoculating a loop full of bacteria in 5 mL of nutrient broth and incubated at 37 ºC for 12 h till a moderate turbidity was developed. Chitosan was dissolved in 5% acetic acid. Polymer concentrations of 1, 1.5 and 2 were prepared for the assay. Bacterial strains *viz*. *Staphylococcus aureus*, *Escherichia coli* and *Bacillus subtilis* were individually swabbed on the Muller-Hilton agar plates and the Nutrient agar plates, respectively. Aseptically, holes were made on the surface of solidified media with the help of a sterile 1 mm tip and into it 100 µL of test sample, *viz.* 1 mg/mL, 1.5 mg/mL and 2 mg/mL, was inoculated. Plates were kept at room temperature for diffusion of the sample for 30 min. The bacterial plates were then incubated at 37 ºC for 24 h. Following incubation, antimicrobial activities were assessed by measuring the diameter of the zone of inhibition [10,11].

Cytotoxicity

Cell culture: Different cell lines such as PSVK1 (normal skin keratinocytes) and MDA MB-231 (triple negative breast cancer) were maintained in complete DMEM (Dulbecco's modified eagle medium) containing 0.1 mM non-essential amino acids, 1.5 g/L sodium bicarbonate, 2 mM l-glutamine and 1.0 mM sodium pyruvate supplemented with 10% fetal bovine serum (FBS; heat inactivated) and 1% antibiotic–antimycotic solution (1000 U/mL penicillin G, 10 mg/mL streptomycin sulphate, 5 mg/mL gentamycin and 25 µg/mL amphotericin B) in 25 and 75 cm^2 mammalian cell culture flasks. The cells were cultured by keeping the flasks in a CO_2 incubator (Heal Force, HF 160 W, Shanghai, China) at 37 ºC, 90% relative humidity, 5% CO_2 and 95% air. When the cells approached 70-80% confluency, they were sub-cultured (passaged) with trypsin–EDTA and fresh medium into 25 cm^2 culture flasks.

Cell proliferation assay: MTT assay was employed to investigate the cytotoxic effect of chitosan at different concentrations on PSVK1 normal skin keratinocytes and MDA-MB-231 triple negative breast cancer cells. Chitosan was disso-

lved in 5% acetic acid in different concentrations such as 10, 25, 50, 100, 150 and 200 µg/mL. 2×10^3 cells were seeded per well in 96-well plates and then incubated for 24 h in a CO_2 incubator under conventional culture conditions (37 ºC, 5% CO_2 and 90% relative humidity). After incubation, cells were treated with different concentrations of chitosan as indicated and incubated for 72 h. 10 µL of 5 mg/mL MTT (Sigma-Aldrich, USA) was added to each well and incubated for 2 h. In case of control, 100 µL of plain medium without the drug was added. The culture medium was discarded and 100 µL of DMSO (Merck, Germany) was added to the wells. The absorbance was then measured at 570 nm in a multimode microplate reader (Spectra Max iD3, Molecular Devices). Percentage proliferation (%P) was calculated using the following formula:

$$P\ (\%) = \frac{\text{Absorbance of treated cells}}{\text{Absorbance of control cells}} \times 100$$

Scratch wound healing assay: A wound-healing (scratch) assay was conducted to assess the impact of chitosan on the migratory capacity of MDA-MB-231 cells. Briefly, MDA-MB-231 cells were seeded at a density of 4×10^5 cells per well in a 12-well plate and cultured until a monolayer was established. To minimize proliferation, the medium was substituted with serum-free 0.1% FBS, followed by incubation for 6 h. Subsequently, a linear scratch was created across the monolayer using a sterile 10 µL pipette tip. The wells were gently washed with 1 x PBS to remove detached cells and treatments were applied with chitosan (5 and 10 µg/mL). Cell migration was monitored at 12 h intervals until complete closure was observed in the control group. Images were captured at 0, 12, 24 and 36 h using a Nikon D5100 digital camera (Nikon, Japan). The wound closure was quantitatively analyzed using ImageJ software (NIH, USA) and the percentage of remaining wound area was calculated and plotted using GraphPad Prism version 9.0.

RESULTS AND DISCUSSION

Total yield: The weight of *Gibelion catla* fish scales before and after treatment, with 50 g of raw scales yielding 4.3 g of chitosan. The chitosan yield was calculated using the standard percentage yield formula:

$$\text{Yield}\ (\%) = \frac{\text{Amount of chitosan obtained}}{\text{Amount of fresh fish scale used}} \times 100$$

Thus, the chitosan yield from 50 g of *G. catla* fish scales was found to be 8.6%, indicating an efficient extraction process and highlighting the potential of fish scale waste as a viable source of chitosan.

FTIR analysis: The FTIR spectrum is shown in Fig. 1. The absorption band observed at 3461 cm^{-1} was attributed to stretching vibrations of OH groups. The band in the region of 1640 cm^{-1} corresponds to stretching vibrations of the C=O bond of carbonyl groups. Absorption band observed at 1471 cm^{-1} can be attributed to the bending vibration of C-H in $–CH_2$. The absorption band observed at 1417 cm^{-1} was attributed to the C–N stretch of secondary amines. The bands at 1020 and 872 cm^{-1} were attributed to stretching vibrations of -CO and vibrations of –C-H in the alkene group. The peak at 562 cm^{-1}

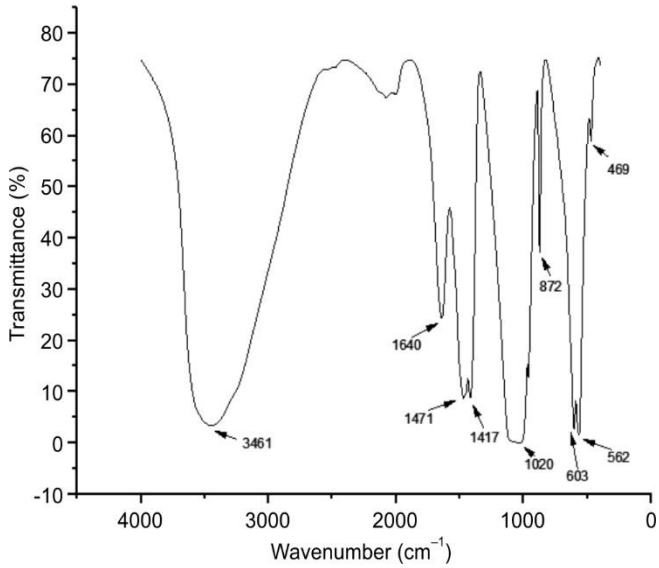

Fig. 1. FT-IR spectrum of fish chitosan

was assigned to NH out-of-plane bending in amide groups [12].

Degree of deacetylation (DDA): The degree of deacetylation of chitosan was also enumerated from the FTIR spectra by the formula DD% = 100 – [(A_{1655}/A_{3450}) × 115] and calculated to be 60.4% [13]. This IR characterization formula of DDA for chitosan relies on the correlation between the absorbance (A) value of the primary amide at 1655 cm^{-1} and that of the hydroxyl at 3450 cm^{-1}.

XRD analysis: The XRD pattern (Fig. 2) around 5-60º shows several peaks with high intensity which indicates the crystalline nature of the chitosan synthesized. The strongest sharp reflection was observed at 2θ around 32.12º. Various characteristic peaks were observed at 2θ values of 25.84º, 46.92º, 49.4º and 53.34º. No specific broad peaks are observed. These results justify that the extracted biomaterial is crystalline in nature. Rasti *et al.* [14] also observed the strong sharp reflection at 2θ around 30-35º for chitosan isolated from the mollusc chiton.

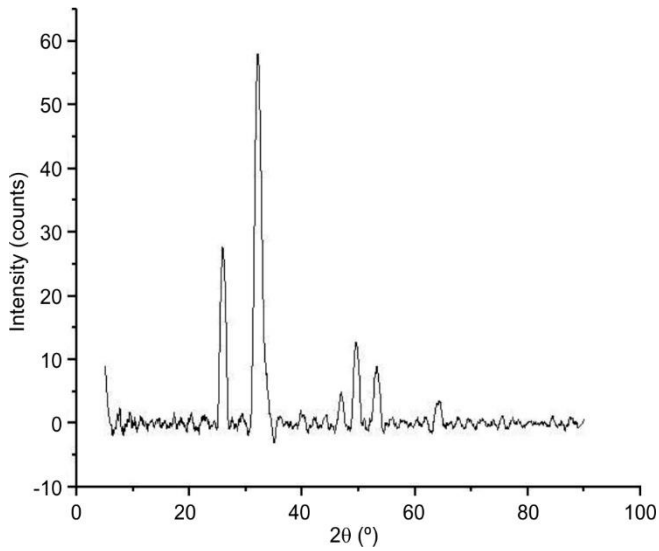

Fig. 2. XRD spectrum of fish chitosan

SEM-EDX: The surface morphology of the prepared chitosan, as observed under SEM, exhibited a coarse texture with visible fibrillar arrangements and intermittent porous zones. These fibrous features were particularly evident in certain regions of the sample, resembling the structural characteristics as reported by Suneeta *et al.* [15]. Comparable morphological patterns such as fragmented flakes and fine fibrils were also noted in crab shell-derived chitosan studied by Yen *et al.* [16], especially under higher magnifications. The SEM image captured at a scale of 10 µm (Fig. 3) highlights these distinct textural elements. The observed porosity suggests that the material may facilitate cellular attachment and growth, indicating its potential utility in wound healing applications [17].

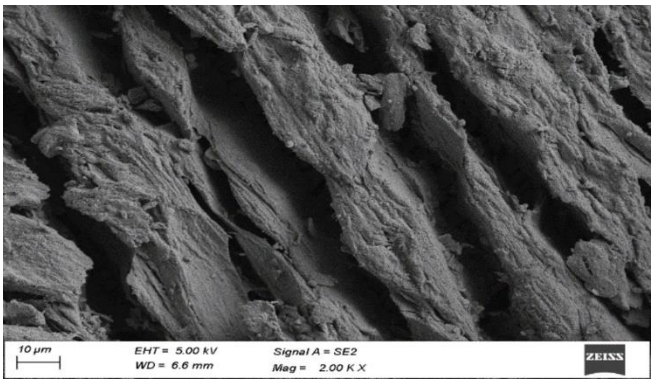

Fig. 3. Scanning electron micrograph of fish chitosan

In addition, Energy Dispersive X-ray (EDX) spectroscopy was employed to assess the elemental profile of the chitosan (Fig. 4). The resulting spectrum identified the presence of elements such as carbon, oxygen, sodium, phosphorus and calcium.

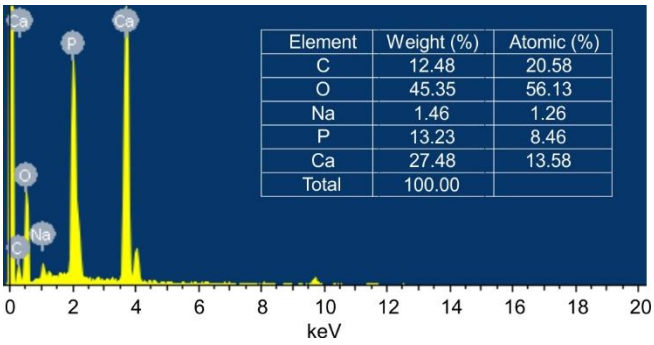

Element	Weight (%)	Atomic (%)
C	12.48	20.58
O	45.35	56.13
Na	1.46	1.26
P	13.23	8.46
Ca	27.48	13.58
Total	100.00	

Fig. 4. EDX spectrum of fish chitosan

Antimicrobial assay: Chitosan exhibited antimicrobial activity against all tested bacterial strains *viz. Escherichia coli*, *Bacillus subtilis* and *Staphylococcus aureus* by exhibiting clear zones of inhibition at all concentrations tested. It was found that the size of the inhibition zones increased with higher chitosan concentrations, indicating a concentration-dependent enhancement in antimicrobial efficacy. Table-1 shows the observed zone of inhibition of isolated chitosan from fish scale at different concentrations. The mechanism of antimicrobial efficacy of chitosan is believed to be due to the interaction of positive charge present in chitosan molecule and negatively charged microbial cell walls. Positively charged amine ($-NH_2$) functional group of chitosan binds with glutamate of the cell membrane protein. It also binds with membrane phospholipids, especially choline, thereby increasing the inner permeability of the membrane, leading to the release of cell fluids in the cytoplasm (lysis) and inhibiting cell division (regeneration) [18]. This mechanism can also explain the increase in antimicrobial efficacy of chitosan with the increase in concentration. When the concentration increases, the number of positively charged amine groups ($-NH_2$) also increases, which can bind to the bacterial cell surface, making it more powerful in obstructing and killing bacteria.

TABLE-1
INHIBITION ZONE OF CHITOSAN AT DIFFERENT CONCENTRATIONS AGAINST *Escherichia coli*, *Staphylococcus aureus* AND *Bacillus subtilis*

Concentration (mg/mL)	*Escherichia coli* (mm)	*Staphylococcus aureus* (mm)	*Bacillus subtilis* (mm)
1.0	25	35	24
1.5	25	40	25
2.0	26	39	25

Cytotoxicity of chitosan: MTT assay was performed to evaluate the cytotoxicity of synthesized chitosan on PSVK1 normal skin keratinocytes and MDA-MB-231 triple-negative breast cancer cells using different concentrations (10 to 200 µg/mL). The MTT assay unveiled no toxic effect for normal skin keratinocytes, while strong cytotoxicity against breast cancer cell lines (Fig. 5). Chitosan suppressed the growth of triple-negative breast cancer cells at a concentration of 200 µg/mL. Gul-e-Saba *et al.* [19] also evaluated the cytotoxic effects of natural chitosan extracted from tilapia fish scales using the MTT assay on various cell lines, including MCF-7 (breast cancer), HepG2 (liver cancer), HeLa (cervical cancer), and 3T3 (fibroblasts). The study reported pronounced cytotoxicity against MCF-7 and HeLa cells, while exhibiting comparatively lower toxicity towards HepG2 and 3T3 cell lines.

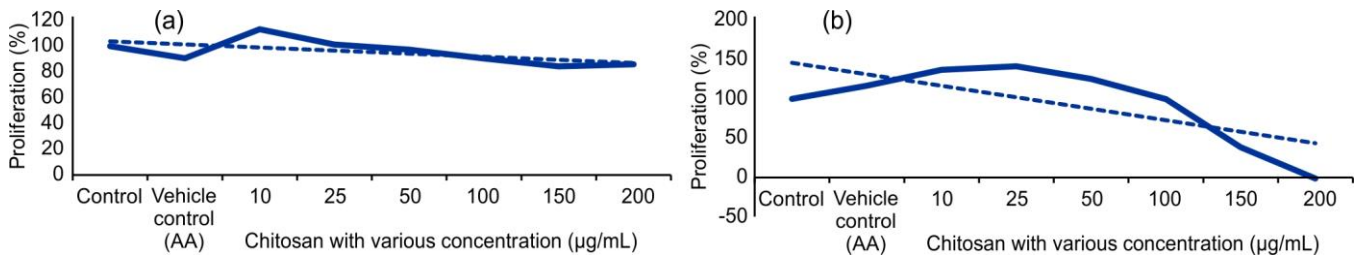

Fig. 5. % Proliferation of chitosan with different concentrations on (a) PSVK 1 cell and (b) MDA MB 231 cell

Wound healing assay: To evaluate the effectiveness of chitosan extracted from the *G. catla* waste as a wound healing material the migratory capacity of MDA-MB-231 upon treatment with chitosan was estimated. At 0 h, a consistent scratch was introduced into the confluent monolayer of MDA-MB-231 cells and wound closure was monitored at regular intervals. Treatment with chitosan resulted in progressive cell migration toward the wound area, with complete closure observed at 36 h post-treatment (Fig. 6). These results suggest that chitosan possesses migratory or wound-healing properties.

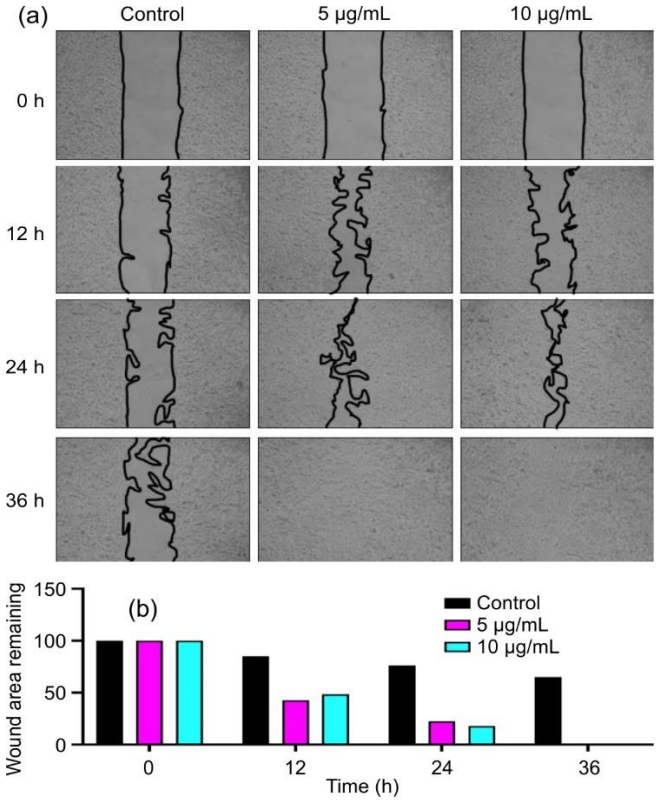

Fig. 6. (a) Migration of chitosan on MDA-MB-231, (b) Graph showing % of wound remaining area at different time interval

Conclusion

This research attempted to isolate chitosan from a natural source (*Gibelion catla* scales), which is basically considered waste. Fish scale is treated chemically and natural chitosan is extracted after demineralization, deproteinization and deacetylation with a yield of 8.6% and achieved a degree of deacetylation of 60.4%, as confirmed by FTIR analysis. The characteristic peaks corresponding to secondary amine and amide groups validated the presence of chitosan. XRD analysis indicated a predominantly crystalline structure, supported by the appearance of sharp, high-intensity peaks and the absence of a broad amorphous band. Morphological analysis through SEM revealed a surface architecture featuring both fibrillary and porous characteristics, while EDX confirmed the elemental composition, including carbon, oxygen, sodium, phosphorus and calcium. Biological evaluation of the extracted chitosan demonstrated significant antimicrobial activity against *Escherichia coli*, *Staphylococcus aureus* and *Bacillus subtilis* with effectiveness increasing proportionally to concentration. The chitosan also exhibited promising anticancer activity, selectively inhibiting the proliferation of MDA-MB-231 (triple-negative breast cancer) cells without inducing toxicity in normal human skin keratinocytes (PSVK-1). Further, chitosan facilitated cell migration in MDA-MB-231 cells, underscoring its potential in promoting wound healing and tissue regeneration. Collectively, these findings highlight the potential of Catla fish scale waste as a sustainable source for bioactive chitosan with multifunctional applications.

ACKNOWLEDGEMENTS

The authors acknowledge Assam down town University for the financial support as a seed grant (AdtU/2022/148).

CONFLICT OF INTEREST

The authors declare that there is no conflict of interests regarding the publication of this article.

REFERENCES

1. H. Izadi, H. Asadi, and M. Bemani, *Front. Mater.*, **12**, 1537067 (2025); https://doi.org/10.3389/fmats.2025.1537067
2. R. Varma and S. Vasudevan, *ACS Omega*, **5**, 20224 (2020); https://doi.org/10.1021/acsomega.0c01903
3. V.P. Santos, N.S.S. Marques, P.C.S.V. Maia, M.A.B. Lima, L.O. Franco and G.M. Campos-Takaki, *Int. J. Mol. Sci.*, **21**, 4290 (2020); https://doi.org/10.3390/ijms21124290
4. J. Nilsen-Nygaard, S.P. Strand, K.M. Vårum, K.I. Draget and C.T. Nordgård, *Polymers*, **7**, 552 (2015); https://doi.org/10.3390/polym7030552
5. C. Casadidio, D.V. Peregrina, M.R. Gigliobianco, S. Deng, R. Censi and P. Di Martino, *Mar. Drugs*, **17**, 369 (2019); https://doi.org/10.3390/md17060369
6. R. Singh, K. Shitiz and A. Singh, *Int. Wound J.*, **14**, 1276 (2017); https://doi.org/10.1111/iwj.12797
7. S. Ahmed and S. Ikram, *Achievements in the life sciences*, **10**, 27 (2016); https://doi.org/10.1016/j.als.2016.04.001
8. D. Brindha, R. Santhi and A. Hemalatha, *Drug Invent. Today*, **10**, 1357 (2018).
9. M.K. Lagat, S. Were, F. Ndwigah, V.J. Kemboi, C. Kipkoech and C.M. Tanga, *Microorganisms*, **9**, 2417 (2021); https://doi.org/10.3390/microorganisms9122417
10. M. Balouiri, M. Sadiki and S.K. Ibnsouda, *J. Pharm. Anal.*, **6**, 71 (2016); https://doi.org/10.1016/j.jpha.2015.11.005
11. S. Purkayastha and P. Dahiya, *Indian J. Pharm. Sci.*, **74**, 443 (2012); https://doi.org/10.4103/0250-474X.108420
12. C. Molina-Ramírez, P. Mazo, R. Zuluaga, P. Gañán and J. Álvarez-Caballero, *Polymers*, **13**, 2079 (2021); https://doi.org/10.3390/polym13132079
13. B. Fatima, in eds.: M. Khan, G.M. do Nascimento and M. El-Azazy, Quantitative Analysis by IR: Determination of Chitin/Chitosan DD, In: Modern Spectroscopic Techniques and Applications, IntechOpen (2020).
14. H. Rasti, K. Parivar, J. Baharara, M. Iranshahi and F. Namvar, *Iran. J. Pharm. Res.*, **16**, 366 (2017); https://doi.org/10.22037/ijpr.2017.1963
15. K. Suneeta, P. Rath and H.K.A. Sri, *Afr. J. Biotechnol.*, **15**, 1258 (2016); https://doi.org/10.5897/AJB2015.15138
16. M.-T. Yen, J.-H. Yang and J.-L. Mau, *Carbohydr. Polym.*, **75**, 15 (2009); https://doi.org/10.1016/j.carbpol.2008.06.006
17. P. Grzybek, Ł. Jakubski and G. Dudek, *Int. J. Mol. Sci.*, **23**, 9932 (2022); https://doi.org/10.3390/ijms23179932
18. A.J. Rahma, D. Kania and I. Taufiqurrahman, *Dentino Jurnal Kedokteran Gigi*, **5**, 53 (2020); https://doi.org/10.20527/dentino.v5i1.8122
19. G.-S. Chaudhry, C.S. Thirukanthan, K.M. NurIslamiah, Y.Y. Sung, T.S.M. Sifzizul and A.W.M. Effendy, *J. Adv. Pharm. Technol. Res.*, **12**, 373 (2021); https://doi.org/10.4103/japtr.japtr_117_21